SCIENTIFIC REPORTS

OPEN

SUBJECT AREAS:
PLANETARY SCIENCE
METEORITICS

Received
5 December 2013

Accepted
17 March 2014

Published
23 April 2014

Microbial mediated formation of Fe-carbonate minerals under extreme acidic conditions

Mónica Sánchez-Román[1], David Fernández-Remolar[1], Ricardo Amils[1,2], Antonio Sánchez-Navas[3], Thomas Schmid[4], Patxi San Martin-Uriz[1], Nuria Rodríguez[1], Judith A. McKenzie[5] & Crisogono Vasconcelos[5]

[1]Centro de Astrobiología (INTA-CSIC), Torrejón de Ardoz, 28850 Madrid, Spain, [2]Centro de Biología Molecular Severo Ochoa, Universidad Autónoma de Madrid, Cantoblanco, 28049 Madrid, Spain, [3]Departamento de Mineralogía y Petrología, Facultad de Ciencias, Universidad de Granada, 18002 Granada, Spain, [4]Department of Chemistry and Applied Biosciences, ETH-Zurich, CH 8093 Zurich, Switzerland, [5]Geological Institute, ETH-Zurich, CH 8092 Zurich, Switzerland.

Correspondence and requests for materials should be addressed to M.S.-R. (msanzroman@cab.inta-csic.es)

Discovery of Fe-carbonate precipitation in Rio Tinto, a shallow river with very acidic waters, situated in Huelva, South-western Spain, adds a new dimension to our understanding of carbonate formation. Sediment samples from this low-pH system indicate that carbonates are formed in physico-chemical conditions ranging from acid to neutral pH. Evidence for microbial mediation is observed in secondary electron images (Fig. 1), which reveal rod-shaped bacteria embedded in the surface of siderite nanocrystals. The formation of carbonates in Rio Tinto is related to the microbial reduction of ferric iron coupled to the oxidation of organic compounds. Herein, we demonstrate for the first time, that *Acidiphilium* sp. PM, an iron-reducing bacterium isolated from Rio Tinto, mediates the precipitation of siderite ($FeCO_3$) under acidic conditions and at a low temperature (30°C). We describe nucleation of siderite on nanoglobules in intimate association with the bacteria cell surface. This study has major implications for understanding carbonate formation on the ancient Earth or extraterrestrial planets.

In the geologic record, evidence for the existence of microorganisms has been observed in sedimentary rocks as old as 3.45 Ga, and their influence on mineral precipitation throughout Earth's history, particularly for carbonate deposits, has been and remains significant[1,2]. However, thermodynamic conditions fundamentally restrict carbonate precipitation to high pH environments (pH $>$ 7), and, in terrestrial environments, the production of carbonates at pH $<$ 4.5 does not occur either by abiotic or biotic mechanisms[3–5]. In spite of this general rule, Fe-rich carbonate minerals have been recently recognized in the subsurface of Rio Tinto in mildly acidic to neutral pH (5–7) and somewhat reducing (Eh $<$ 0) conditions[6,7]. Rio Tinto is an acid-sulphate system considered as one of the potential analogues for life on early Earth and Mars[7]. *Acidiphilium* species are very abundant in Rio Tinto[8], these *alphaproteobacteria* can grow on organic compounds under microaerobiosis and anaerobic conditions using ferric iron (Fe^{3+}) and/or oxygen as electron acceptors[9,10]. In this study, we conducted culture experiments with *Acidiphilium* species to investigate the mediation of carbonate precipitation under low pH and temperature conditions. We present a high-resolution transmission electron microscopy (TEM), atomic force microscopy (AFM), scanning electron microscopy (SEM) and Raman spectroscopy study of the microbial carbonate precipitates (see methods section). We propose that the direct mediation of acidophilic microorganisms can overcome kinetic barriers to carbonate formation and that they may play an active role in the formation of carbonates in acidic and natural environments.

The culture experiments were designed with an iron-reducing bacterium, *Acidiphilium* sp. PM, and incubated at 35°C in acidic media for 45 days. To identify crystal precipitates, the cultures were observed periodically with optical microscope. We measured the pH at the end of the culture experiments. Parallel control experiments without bacteria and non-viable cells were run. Using a combination of Raman, sensitive energy dispersive X-ray Spectroscopy (EDS), TEM, SEM and AFM analyses, we have identified the mineral composition and investigated the involvement of *Acidiphilium* sp. PM in the nucleation of carbonates. Our research demonstrates that bacteria can create chemical microenvironments in the region directly surrounding their cell walls, and, thus, can

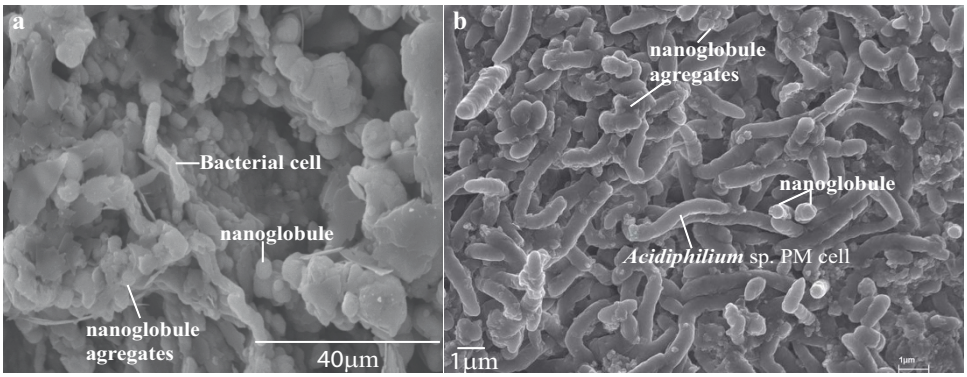

Figure 1 | SEM images of Rio Tinto basin sediment (a) and siderite nanoglobules from culture experiments (b) showing granulated texture. (a) Mineralized rod-shape bacteria from the Rio Tinto sediment in intimate association with siderite nanoglobules. (b) Nanoglobules attached to the *Acidiphilium* sp. PM cells. These nanoglobules range from 30 to 100 nm. Note that the morphology and size of those observed rod-shape bacteria in Rio Tinto sediment are in accordance with the morphology and size of the *Acidiphilium* sp. PM cells.

effectively produce spatially restricted supersaturated conditions in which otherwise unpredicted minerals can precipitate.

Results

No precipitation was observed in non-viable cell and cell-free control experiments. *Acidiphilium* sp. PM reduced 94% of the Fe^{3+} present in the medium. The starting concentration of Fe^{3+} was 1.33 g/L and the final concentration 0.04 g/L.

AFM and TEM observations show mineral precipitates less than 200 nm in diameter (termed nanoglobules[11,12]) with an irregular size and distribution (Figs. 2,3). Most of the nanoglobules are 20–100 nm in size while the remaining globules are 100–200 nm (large nanoglobules). The nanoglobules are composed of Fe-carbonate, most likely siderite based on Raman and EDX analyses (Figs. 4a,5), and occur attached to the surface of *Acidiphilium* sp. PM cells, where they are in some cases embedded in a thin organic film that surrounds the cells (Fig. 2). This organic film is produced by *Acidiphilium* sp. PM during growth and is composed of EPS as demonstrated by Raman spectroscopy analyses (Fig. 4b). In detailed view, we can observe that the surface of *Acidiphilium* sp. cells is surrounded by nanoglobules (Figs. 2b,c).

Figure 4a shows average of three Raman spectra collected from nanoglobules formed in culture experiments and the spectra of a siderite standard taken from Somorrostro (Vizcaya, Spain). The spectra were collected with an acquisition time of 60 s each. For precise positioning, an AFM tip was put on a nanoglobule, and the laser beam of a combined AFM-confocal Raman setup (see Methods) was focused onto the tip apex. All sample spectra contain Raman band at 520 cm^{-1} assigned to the Si-Si stretching vibration of the AFM tip material. The band at 1087 cm^{-1} is the most prominent band in the Raman spectrum of siderite (Fig. 4a). The band at 1087 cm^{-1} in both spectra (nanoglobules and reference material) is in good agreement with the symmetric stretching vibration of CO_3^{2-} (γ_1) in siderite as described previously[13,14].

Discussion

Bacterial nucleation and precipitation of carbonate. Our AFM, TEM and SEM studies demonstrate that siderite crystals nucleate on baterial nanoglobules, as previously suggested for Ca and/or Mg-carbonate precipitation[11,12]. The initial steps of nanoglobule formation occur in the outer side of the bacterial envelopes and in some cases within an organic film composed of exopolysaccharides (EPS) in intimate association with the bacteria cell surface (Figs. 2,4b). Because EPS have the capacity of binding metal ions, the organic film may serve as a site for globule nuclei formation[15,16] in addition to the bacterial outer membrane. These experimental findings show that metabolically active, acidophilic, Fe-reducing

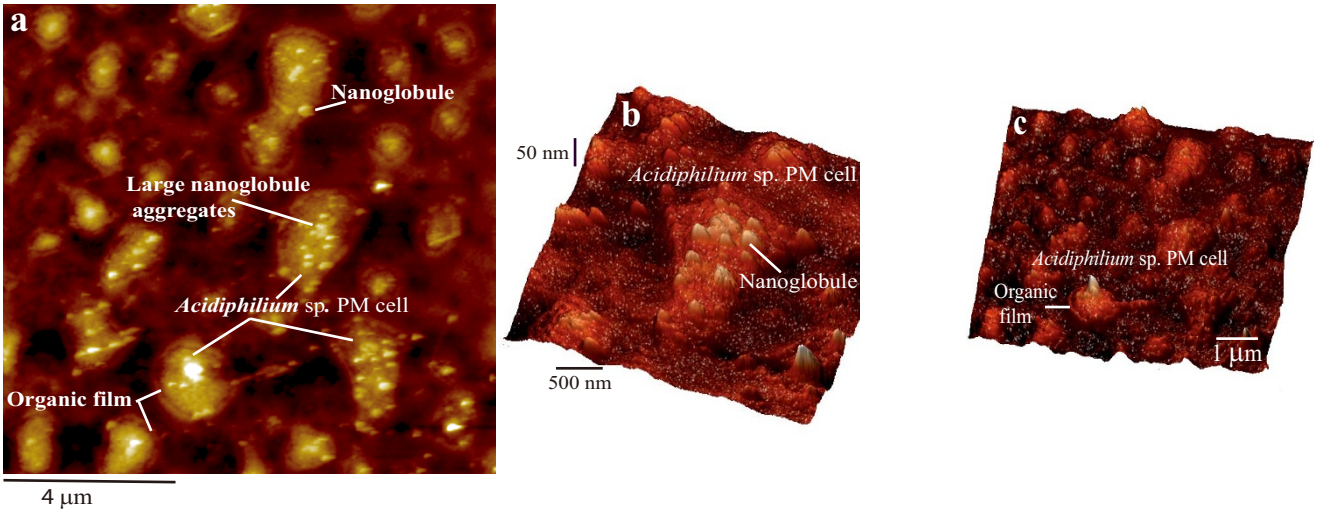

Figure 2 | AFM of siderite nanoglobules formed in *Acidiphilium* sp. PM cultures. (a) General AFM view showing aggregates of nanoglobules attached to *Acidiphilium* sp. cell. Most of field is occupied by aggregates of large globules. (b), (c) Detail of *Acidiphilium* sp. PM cell covered by nanoglobules (<100 nm), which are embedded in a thin organic film.

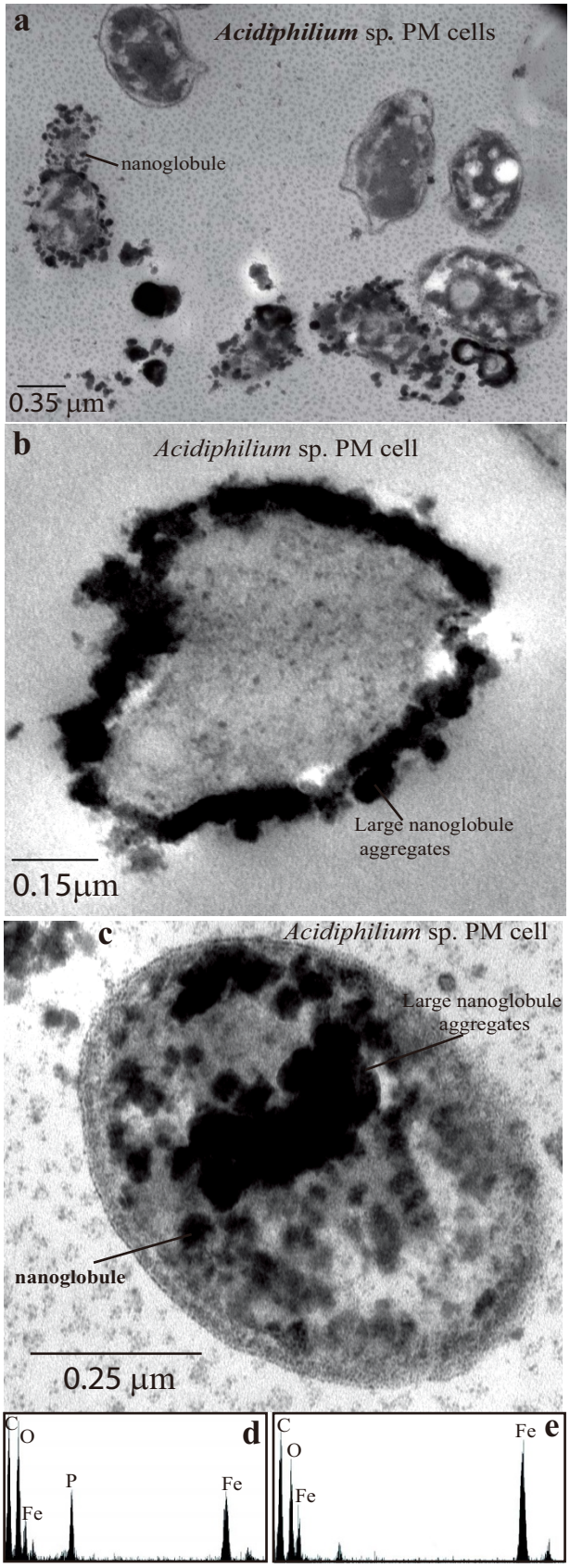

Figure 3 | TEM of siderite nanoglobules formed in *Acidiphilium* sp. PM cultures. (a) TEM overview showing *Acidiphilium* sp. PM cells covered by nanoglobules. (b), (c) Detail of *Acidiplilium sp.* PM cell in intimate association with large and small nanoglobules. (d) EDX spectrum of lighter mineralized areas composed of Fe-carbonate with some P. (e) EDX spectrum nanoglobules (dark areas) which are composed of Fe-carbonates.

bacteria are capable of producing conditions that promote the nucleation of Fe-carbonate under acidic conditions.

The nanoglobules attached to the bacteria cell surfaces (Figs. 2,3) and some mineralized bacteria within the siderite crystals (Figs. 1,5) provide evidence that bacterial precipitation of siderite may begin with the accumulation of Fe in the external bacterial envelopes and/or in the organic film and be followed by precipitation as nanoglobules on the cell surface. Based on the results of our culture experiments, we propose that the presence of acidophilic bacteria can mediate carbonate precipitation under acidic conditions and overcome the kinetic barrier to its formation by creating neutral to alkaline conditions in the microenvironment surrounding bacterial cells. It is well known that bacteria are capable of changing physico-chemical conditions (e.g., pH, CO_2, metal ion concentration) in their surrounding microenvironment[2,17–22]. Thus, carbonate minerals that are undersaturated in abiotic medium can precipitate because bacteria concentrate around their cells the ions of interests, in this case Fe^{2+} and CO_3^{2-}, until supersaturation is reached[18]. There is a bacteria-medium interface in which reaction mechanisms change and thermodynamic activation energies can be modified leading to the precipitation of minerals[17,19]. Therefore, pure aqueous solution chemistry cannot be applied to study such bacterial precipitating microenvironments[19–22]. Abiotic mineral precipitation does not occur in natural systems or in sterile laboratory experiments unless thermodynamic conditions are favourable[2–5,22]. However, in a biotic medium, bacteria induce mineral precipitation (1) by modifying the conditions of their surrounding environment and/or concentrating ions in the bacterial cell envelope and (2) by acting as nucleation sites[20–24]. For instance, as we show here, iron-reducing bacteria are capable of precipitating carbonates under acidic conditions by neutralizing the pH and lowering the Fe^{3+}/Fe^{2+} ratio locally.

Table 1 shows the mineral saturation index (SI) values for the initial conditions of the culture medium assayed. These values indicate that the medium is undersaturated with respect to anhydrite, calcite, dolomite, siderite and vivianite. This geochemical modelling suggests that the physico-chemical conditions of the medium are favourable to promote the abiotic precipitation of jarosite, goethite, hematite and strengenite. However, none of these mineral phases were observed in our cultures. Hence, we conclude that *Acidiphilium sp.* control the processes of mineral precipitation. Its metabolic activity creates a microenvironment enriched in Fe^{2+}, CO_2, NH_3 and PO_4^{3-}, i.e., suitable for the precipitation of Fe^{2+}-rich minerals (e.g., siderite) instead of Fe^{3+} minerals (e.g., jarosite, hematite, goethite and/or magnetite).

Mechanism of precipitation of carbonate. The formation of iron carbonates is an equilibrium or kinetic process controlled by the concentration of Fe^{2+} and CO_3^{2-} in solution[25]. Previous studies suggested[25] that the production of large amount of siderite requires high concentration of Fe^{2+}, which can be obtained by bacterial reduction of Fe^{3+}. Therefore, the occurrence of siderite in Earth's surface sedimentary environments could be favoured by iron reducing bacteria. On the other hand, mineralization can taken place on the wall or on the surface of the bacterial cells that are presumably sheathed by extracellular polysaccharides[23,24,26,27]. In this study, the surface of *Acidiphilium* sp. PM provides sites for nucleation of Fe-phosphate after adsorbing Fe^{2+} into cellular envelopes and its EPS. Nucleation would start by binding Fe^{2+} to the phosphate groups of the outer membrane (mainly phospholipids and lipopolysaccharides). This promotes the formation of transient amorphous ferrous phosphate (AFP) phases (Fig. 3).

Microbes promote the precipitation of carbonate minerals metabolically either by increasing the pH and the alkalinity of their surrounding microenvironment or by the secretion of substances that facilitate the mineral nucleation[11,12,15,16,24,26]. In the Precambrian, heterogeneous nucleation on bacterial cell surfaces, apparently, exerted

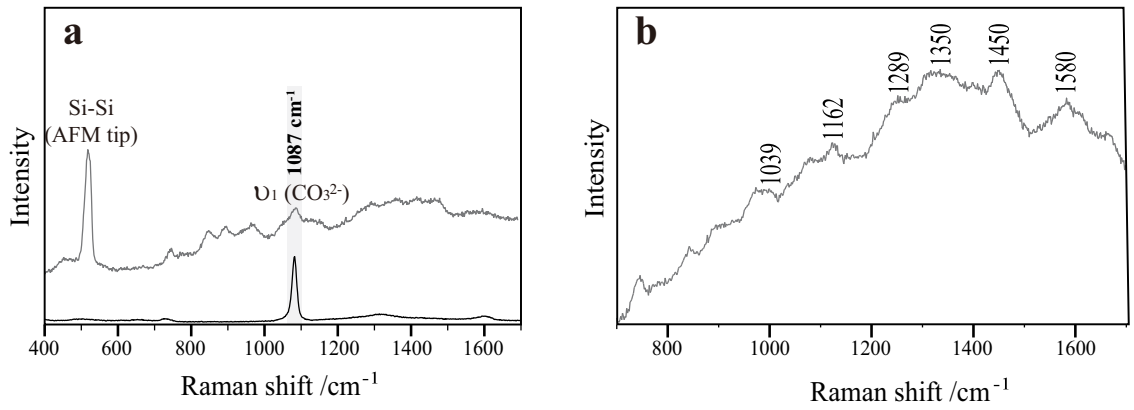

Figure 4 | (a) Raman spectra of both nanoglobules formed in *Acidiphilium* sp. PM culture experiments and siderite standard (reference material). (b) Raman spectrum of the extracellular organic film (EPS). See main text and methods for band assignments.

a powerful control on carbonate formation[28,29]. Nucleation of carbonate minerals on organic surfaces (i.e., heterogeneous nucleation) can occur when negatively charged surface groups such as carboxylate, phosphate, and sulphate complexes bind divalent metal cations (e.g., Ca, Mg, Fe, Mn). Furthermore, this nucleation can increase the number of crystal nuclei even when the bulk medium is supersaturated with the mineral carbonate phase by more than an order of magnitude[28]. Heterogeneous nucleation can take place on the microbial cell surfaces and envelopes, or within the exopolymeric matrix surrounding the cells.

Nucleation on bacterial cells depends on the surface charge, which is controlled both by structural features of cell wall and by bacterial metabolism[23,24,26,27,30]. Our data confirm that the formation of siderite is controlled by (1) the Fe^{2+} concentration on the surface of living bacterial cells, driving the precipitation of Fe-rich phosphate precursors and (2) the bacterial metabolic activity, as previous studies have shown for the formation of calcium carbonate[27]. After the bacterial metabolic release of CO_2, three chemical species form in the aqueous solution (H_2CO_3, HCO_3^- and CO_3^{2-}), for which the partitioning is governed by the pH[5]:

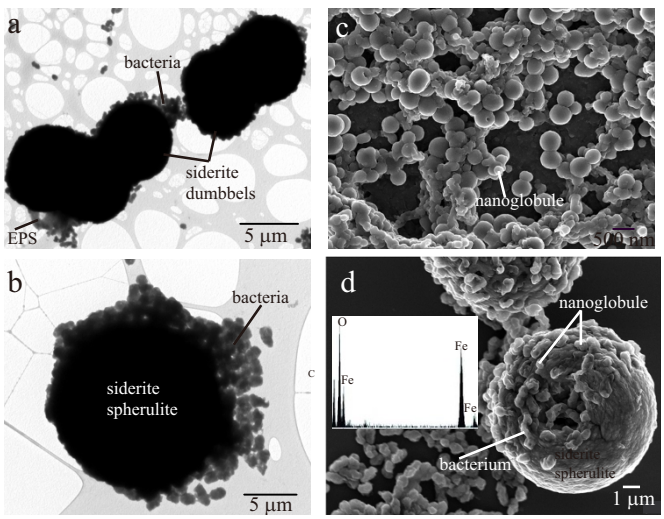

Figure 5 | **TEM (a), (b) and SEM (c), (d) images of siderite precipitates formed in *Acidiphilium* sp. PM cultures.** (a), (b) siderite dumbbells and spherulite covered by bacteria (*Acidiphilium* sp. PM). (c) overall view of siderite nanoglobules. (d) detail of the surface of a microspherulite of siderite with mineralized bacteria resting on nanoglobular crystals. These microspherulites were formed after 45 days of incubation. The insert of the EDX analysis of the microspherulite demonstrate that it is 100% Fe-carbonate.

$$CO_2 + H_2O \leftrightarrow H_2CO_3 \leftrightarrow HCO_3^- + H^+ \leftrightarrow 2H^+ + CO_3^{2-} \quad (1)$$

Partitioning of HCO_3^- and CO_3^{2-} in Fe-rich environments responsible for Fe-carbonate supersaturation is explained by the reaction:

$$CO_2 + H_2O + FeCO_{3(solid)} \leftrightarrow 2HCO_3^- + Fe^{2+} \quad (2)$$

Reactions (1) and (2) show that the increase in CO_2 promotes dissolution of carbonate minerals to form soluble bicarbonate. Nevertheless, the precipitation of Fe-carbonate (siderite) from CO_2-rich solutions in the presence of Fe^{2+} is promoted by the higher concentration of the CO_3^{2-} with respect to HCO_3^- and H_2CO_3 at neutral to alkaline pH[5,27,31]. In the present study, the pH of the medium was 3.5 throughout the experiment; however, a change in pH was observed at the site of mineral precipitation, *i.e.*, bacterial-medium interface, where the pH was in the range of 6–7. The Fe source used in this study is Fe^{3+} sulphate, which was reduced to Fe^{2+} by the bacteria.

The alkalinisation necessary for $FeCO_3$ precipitation is promoted by the presence of chemical species close to the cell boundary that could act as proton sinks. As the medium contains amino acids, the alkalinisation could be induced due to NH_3 production in the microenvironment around cells. This scenario allows us to explain the observed increase of pH from 3.5 to 6–7 at the bacterial-medium interface (site of mineral precipitation). We propose the following mechanism of precipitation. Besides CO_2 and NH_3 close to the cells, bacterial oxidation of the organic compounds also supplies abundant PO_4^{3-} ions that concentrate first around bacterial cells[27]. Phosphate ions and particularly ammonia are hydrolysed in the same way as CO_2[27] with the subsequent increase of the pH in the microenvironment around cells according to the following reactions:

$$NH_3 + H_2O \rightarrow NH_4^+ + OH^- \quad (3)$$

$$PO_3^- + H_2O \rightarrow HPO_4^{2-} + OH^- \quad (4)$$

$$HPO_4^{2-} + H_2O \rightarrow H_2PO_4^- + OH^- \quad (5)$$

As the growth medium contains more nitrogen than phosphorous, the role of reaction (3) in the neutralization and alkalinisation is more significant than that of reactions (4) and (5). Excess of PO_4^{3-} around bacterial cells provides binding sites for Fe^{2+}, apart from those available from phospholipids of the outer bacterial membranes, allowing amorphous Fe phosphate supersaturation and its kinetically-favoured precipitation close to bacterial surfaces[27]. The involvement of phosphate precursors in biomineralization processes is well known[32–35]. It should be noticed that CO_3^{2-} ions hinder the precipitation of phosphate minerals[36,37], while PO_4^{3-} ions hinder the

Table 1 | Saturation index values (SI) in all media assayed. Results are from geochemical computer program PHREEQC. These SI values are for initial conditions

Mineral phase	SI
Anhydrite, $CaSO_4$	−1.07
Gypsum, $CaSO_4$	−1.14
Aragonite, $CaCO_3$	−7.91
Calcite, $CaCO_3$	−7.77
Dolomite, $CaMg(CO_3)_2$	−15.10
Siderite, $FeCO_3$	−4.58
Jarosite, $KFe_3(SO_4)_2(OH)_6$	11.61
Lepidocrocite, FeOOH	2.52
Goethite, FeOOH	3.56
Magnetite, Fe_3O_4	7.73
Hematite, Fe_2O_3	12.16
Strengite, $FePO_4 \times 2\ H_2O$	3.76
Vivianite, $Fe_3(PO_4)_2 \times 8H_2O$	−7.88

precipitation of carbonate minerals[38,39]. Therefore, NH_3 and PO_4^{3-} act as proton sinks, and their protonation promotes both alkalinisation and conversion of CO_2 into CO_3^{2-}. Indeed, in our culture experiments the precipitation of Fe-phosphate removes PO_4^{3-} ions from the medium, leading to the precipitation of Fe-carbonate.

We have found similar nanometer-sized spheres with granulated texture in Fe-carbonate samples from the Rio Tinto basin (Fig. 1a). Their occurrence is likely related to microbial mediation[10,11] as observed for siderite formed in *Acidiphilium* cultures grown in microaerobiosis (Figs. 1b,2,3,5) and for other carbonates formed in anaerobic and aerobic cultures[11,12,15,16]. After 45 days of incubation, the nanoglobules appear to coalesce into microspherulite structures (Fig. 5). The preservation of such structures in the rock record could provide a tool to trace microbial processes through geologic time. In fact, similar nanometer spheres have been found in Triassic and Proterozoic carbonates[12,40–42] as well as in modern carbonate formation environments[12,43,44].

Understanding the evolutionary sequence of minerals associated with Earth's evolving microbial communities can provide clues and possibly new proxies to evaluate the existence of life on other planets, which might be found associated with specific mineral assemblages[45]. Accordingly, the formation of Fe-carbonate nanoglobules on the cell surface of *Acidiphilium* sp. PM reveals an unexplored pathway for carbonate mineralization under acidic conditions and adds a significant dimension to the study of Martian biogenic activity using terrestrial analogues such as Rio Tinto. For example, it seems that a sulphate- and iron-enriched acidic ocean dominated the surface of early Mars[46–50]. Additionally, the formation of Fe-carbonate by Fe^{3+}-reducing bacteria may play an important role in Fe and C biogeochemistry in natural environments. Finally, these culture experiments may provide valuable insight into understanding the origin of Archean Fe-carbonates[51–55].

Methods

Microorganism. *Acidiphilium* sp. strain PM (DSM 24941) was isolated from the acidic, heavy metal-rich waters of Rio Tinto[10]. As other members of this genus, it is a strict acidophile and a facultative aerobe. It grows on organic matter using O_2 or Fe^{3+} as electron acceptors. This Fe^{3+} respiration (dissimilatory reduction) can be achieved both in aerobiosis and in microaerobiosis.

Culture medium. *Acidiphilium* sp. PM was grown in S-1 medium, with the following composition, (%, wt/vol): 0.2% $(NH_4)_2SO_4$; 0.01% KCl; 0.03% $K_2HPO_4 \times 3H_2O$; 0.025% $MgSO_4 \times 7H_2O$; 0.002% $Ca(NO_3)_2 \times 4H_2O$; 0.1% yeast extract; 0.05% proteose peptone; 0.1% glucose, 0.2% $NaHCO_3$ and 0.5% $Fe_2(SO_4)_3 \times H_2O$. To obtain a solid medium, 2% Bacto-Agar was added. pH was adjusted to 3.5 with 0.1 M H_2SO_4 and the solution was sterilized at 121°C for 20 minutes.

Study of crystal formation. *Acidiphilium* sp. PM was surface-inoculated in Petri-dishes incubated aerobically at 35°C. Up to 45 days after inoculation, the cultures were examined periodically for the presence of minerals using a light microscopy (20×). The experiments were carried out in triplicate. Controls consisting of uninoculated culture media and media inoculated with autoclaved (non-viable) cells were included in all experiments. pH measurements were performed at the end of the growth and mineral formation experiments. pH-indicator paper (Merck Spezial-Indikatorpapier) was directly applied on the semi-solid surface. In situ fluorescence hybridization using a specific probe designed for *Acidiphilium* sp. (LEP636) was used to ensure the purity of the cultures.

To collect the precipitate, the colonies were scraped from the agar surface after an incubation period of 45 days. The collected material was washed several times with distilled water to remove the nutritive solution and any retained agar or cellular debris. The precipitates were then dried at 37°C and microscopic examination showed that this treatment did not alter the crystal morphology.

Scanning electron microscopy (SEM); transmission electron microscopy (TEM); atomic force microscopy (AFM) and Raman spectroscopy analyses. The microbial precipitates from culture experiments were analyzed with a field emission SEM equipped with an electron dispersive detector (EDS) (Leo 1530, 143 eV resolution, LEO Electron 64 Microscopy LTD, Germany).

Microbial precipitates were analyzed by TEM, AFM and Raman microscopy after 20 and 45 days of incubation, respectively, when the crystal precipitates were visible by optical microscopy. Sub-samples were prepared by scraping a small quantity of the bacteria off of the culture plates with a sterile loop and transferring it into a centrifuge tube containing nanopure water. After centrifugation at 3000 g for 10 minutes the supernatant was discarded and cells were resuspended in fresh nanopure water. This washing procedure was repeated three times.

For TEM analyses, a drop of resuspended subsample was pipetted onto collodium/carbon-coated mesh copper grids and air-dried for 1–2 hours. The samples were analyzed using a Philips CM 20, 200 KV, equipped with an EDX model EDAX system (EDAX Inc., Mahwah, NY, USA) for microanalysis. Mica disks were cleaved several times to obtain thin individual disks. A drop of subsample was placed on a mica disk and was allowed to stand for 30 minutes, and air dry before imaging in air. Analytical electron microscopy microanalyses in scanning transmission electron microscopy mode were performed using a 5 nm beam diameter and a scanning area of 1000 × 20 nm.

Samples for AFM and Raman microspectroscopy were prepared by scraping off a small amount from the surface of a culture plate and resuspending aggregates consisting of bacteria, EPS and nanoglobules in DI water. The suspension was drop-coated onto a glass slide and dried under a stream of N_2 gas. For both, AFM and Raman analyses an NTEGRA Spectra Upright system from NT-MDT (Zelenograd/Moscow, Russia) was employed. The system is fiber-optically coupled with a 532-nm diode-pumped solid state (DPSS) laser and equipped with a white-light microscopy module with CCD camera for sample observation, a photomultiplier tube (PMT) detector for registration of laser light that was back scattered by the sample and a spectrometer with four interchangeable gratings and a CCD detector (Newton, Andor, Belfast, Northern Ireland/UK) for collection of Raman spectra. All optical and spectroscopic experiments are performed by using a 100×/N.A. = 0.7 objective with approx. 10 mm working distance for both, focusing light onto the sample and collecting light backscattered from the sample. Within the working distance of the objective, modules for atomic force (AFM) or scanning-tunnelling microscopy (STM) can be placed between sample and objective lens. The system allows both sample scanning for AFM/STM and spectroscopic measurements as well as laser scanning for spectroscopic measurements. All measurements were controlled and data were analysed using NT-MDT's Nova software. A detailed description of the system is available[56].

AFM images with 256 × 256 pixels on sample areas down to 500 × 500 nm^2 were performed in semi-contact mode using specially shaped 'nose-type' silicon cantilever tips (AdvancedTEC, Nanosensors, Neuchatel, Switzerland) allowing for focusing laser light onto the tip end from top with the AFM probe in close proximity to the sample. For collecting Raman spectra on dedicated spots of these highly heterogeneous samples, the tip was placed on the sample after collection of an AFM image and the laser spot was aligned to the tip apex by using the laser-scanning mode. The tip apex was identified on both PMT images revealing the shape of the tip end and Raman images collected in laser-scanning mode by searching for the strongest Raman signal at 520 cm^{-1}. This band is assigned to the main lattice vibration of silicon, the material the AFM tip is composed of. This procedure allows collecting Raman spectra from sample structures (e.g. dense aggregates of nanoglobules) that have been identified on AFM images. Accordingly, all sample spectra presented here contain the silicon band at 520 cm^{-1}. In order to reduce its intensity, in some measurements the laser spot was moved up to 1 μm away from the tip along the tip axis, still allowing for placing the measurement spot onto dedicated structures identified in the AFM images. Raman spectra were collected with a laser power of approx. 1 mW at the sample (λ = 532 nm) and a collection time of 60 s (sum of 6 accumulations of 10 s each).

For identification of siderite in these heterogeneous samples, reference spectra of siderite were collected with the same instrument using the same measurement parameters. The spectrometer calibration was checked on each measurement day by collecting spectra of a silicon waver and diamond particles on a grinding paper. Small deviations from the ideal spectrometer calibration were corrected by moving the central pixel of the spectrum in the way that the main silicon band appeared at 520 cm^{-1} and the most prominent diamond band at 1330 cm^{-1}. Reference spectra were collected from siderite powder taken from Somorrostro (Vicaya, Spain) (532 nm, approx. 1 mW, 60 s). The exact same position of the most prominent band

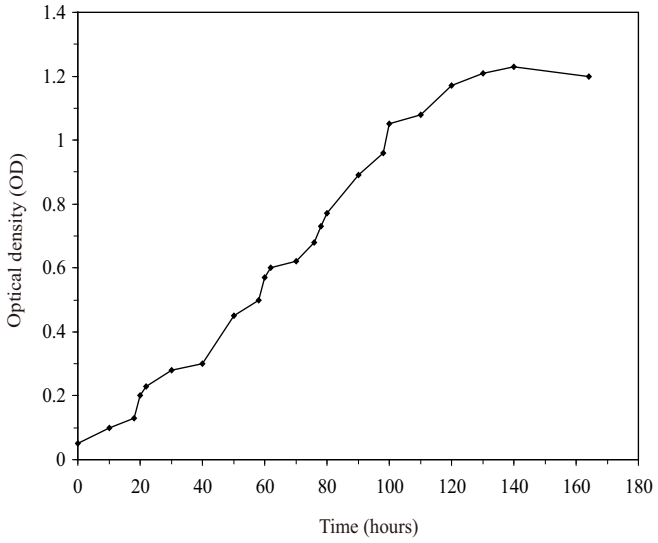

Figure 6 | Growth curve of *Acidiphilium* sp. PM in S-1 medium.

for siderite and a band present in all sample spectra at 1087 cm^{-1} (Fig. 2d) confirms the presence of siderite in the bacteria samples.

In addition to the Raman bands at 520 cm^{-1} (silicon) and 1087 cm^{-1} (siderite) the sample spectra are dominated by a strong and spectrally broad fluorescence background and contain several additional sharp Raman bands. These features can be generally assigned to organic material (bacteria, EPS or remaining agar from the culture plates), see Figure 4b. Also, in many different organic/biological systems, a broad signal in the range of 1250–1350 cm^{-1} can be found, which is a superposition of =C-H bending and CH_2 twisting vibrations with contributions from the amide III mode[57–59] and is represented in our case by the signal at 1289 cm−1. The range between 1000 and 1200 cm^{-1} is characterized by C-C single bond stretching vibrations and contributions from C-N and C-O vibrations. The band at 1162 cm−1 is most probably the C-C single bond vibration corresponding to the 1577 cm^{-1} C=C vibration of conjugated double bond systems[55]. For the sharp bands at 1125 and 1039 cm−1 an assignment to both, C-C of organic material and carbonate stretching vibrations of minerals is possible. The band at 1039 cm^{-1} represents probably an unknown/amorphous form of a carbonate mineral or represents C-C stretching vibrations of organic material. Typical bands present in the spectra of many organic molecules are, for example, various C-H bending modes adding up to a broad band at approx. 1450 cm^{-1} (band labelled in Fig. 4b). The broad bands at 1350 cm^{-1} and 1580 cm^{-1} can also be due to organic material or be explained by the presence of amorphous carbon in the samples.

Geochemical modelling. The activity of dissolved species and the degree of saturation for specific minerals (saturation index, SI) in the culture medium were determined using the geochemical computer program PHREEQC version 2[60]. SI is defined by SI = log (IAP/Ksp), where IAP is the ion activity product of the dissolved mineral constituents and Ksp is the solubility product of the mineral. Thus, $SI < 0$ implies oversaturation with respect to the mineral, whereas $SI > 0$ implies undersaturation.

Growth curve and Fe^{2+} measurements. Liquid cultures were carried out in 500-mL Erlenmeyer flasks containing 200 mL of S-1 medium. Bacterial growth was evaluated by following changes in the optical density (OD) at a wavelength of 600 nm (Fig. 6) using a Spectronic 20 Genesys spectrophotometer. The Fe^{2+} was measured using a RQflex 10 Merck reflectoquant.

1. Bontognali, T., Sessions, A. L., Allwood, A. C., Fischer, W. W. & Grotzinger, J. P. *et al.* Sulfur isotopes of organic matter preserved in 3.45-billion-year-old stromatolites reveal microbial metabolism. *Proc. Natl. Acad. Sci.* **109**, 15146–15151 (2012).
2. Ehrlich, H. L. & Newman, D. K. *Geomicrobiology, 5th Edition* (Marcel Dekker, New York, 2009).
3. Sánchez-Román, M., Fernández-Remolar, D., Amils, R. & Rodriguez, N. Microbial mediation of Fe-Mg-Ca carbonates in acidic environments (Rio Tinto): field studies vs culture experiments. *Goldschmidt Conference* Abstract **A905** (2010).
4. Morse, J. W. & Arvidson, R. S. The dissolution kinetics of major sedimentary carbonate minerals. *Earth Sci. Rev.* **58**, 51–84 (2002).
5. Stumm, W. & Morgan, J. J. *Aquatic Chemistry, Chemical Equilibria and Rates in Natural Waters, 3rd Edition* (John Wiley & Sons, Inc., New York, 1996).
6. Fernández-Remolar, D. C. *et al.* Underground habitats in the Río Tinto basin: a model for subsurface life habitats on Mars. *Astrobiology* **8**, 1023–1047 (2008).
7. Fernández-Remolar, D. C. *et al.* Carbonate precipitation under bulk acidic conditions as a potential biosignature for searching life on Mars. *Earth. Planet. Sci. Lett.* **351–352**, 13–26 (2012).
8. Garcia-Moyano, A., Gonzalez-Toril, E., Aguilera, A. & Amils, R. Comparative microbial ecology study of the sediments and the water column of the Rio Tinto, an extreme acidic environment. *FEMS Microbiol. Ecol.* **81**, 303–314 (2012).
9. Brenner, D. J., Krieg, N. R., Staley, J. T. & Garrity, G. M. *Bergey's Manual of Systematic Bacteriology, 2nd Edition* vol. **2**, part B (Springer, New York, 2005).
10. San-Martin-Uriz, P., Gómez, M. J., Arcas, A., Bargiela, R. & Amils, R. Draft genome sequence of the electricigen Acidiphilium sp. Strain PM (DSM 24941). *J. Bact.* **193**, 5585–5586 (2011).
11. Aloisi, G. *et al.* Nucleation of calcium carbonate on bacterial nanoglobules. *Geology* **34**, 1017–1020 (2006).
12. Sánchez-Román, M. *et al.* Aerobic microbial dolomite at the nanometer scale: implications for the geologic record. *Geology* **36**, 879–882 (2008).
13. Buzgar, N. & Apopei, A. I. The Raman study on certain carbonates. *Geologie Tomul L.* **2**, 97–112 (2009).
14. Isamber, A., Valet, J. P., Gloter, A. & Guyot, F. Stable Mn-magnetite derived from Mn-siderite by heating in air. *J. Geophys. Res.* **108**, 2283 (2003).
15. Bontognali, T. R., Vasconcelos, C., Warthmann, R., Dupraz, C., Bernasconi, S. & McKenzie, J. A. Microbes produce nanobacteria-like structures, avoiding cell entombment. *Geology* **36**, 663–666 (2008).
16. Krause, S. *et al.* Microbial nucleation of Mg-rich dolomite in exopolymeric substances under anoxic modern seawater salinity: New insight into an old enigma. *Geology* **40**, 587–590 (2012).
17. Ahimou, F., Denis, F. A., Touhami, A. & Dufrene, Y. F. Probing microbial cell surface charges by atomic force microscopy. *Langmuir* **18**, 9937–9941 (2002).
18. Párraga, J. *et al.* Study of biomineral formation by bacteria from soil solution equilibria. *React. Funct. Polym.* **36**, 265–271 (1998).
19. Thompson, J. B. & Ferris, F. G. Cyanobacterial precipitation of gypsum, calcite, and magnesite from natural alkaline lake water. *Geology* **18**, 995–998 (1990).
20. Warthmann, R., van Lith, Y., Vasconcelos, C., McKenzie, J. A. & Karpoff, A. M. Bacterially induced dolomite precipitation in anoxic culture experiments. *Geology* **28**, 1091–1094 (2000).
21. van Lith, Y., Warthmann, R., Vasconcelos, C. & McKenzie, J. A. Sulphate-reducing bacteria induce low temperature dolomite and high Mg-calcite formation. *Geobiology* **1**, 71–79 (2003).
22. Sánchez-Román, M. *et al.* Aerobic biomineralization of Mg-rich carbonates: Implications for natural environments. *Chem. Geol.* **281**, 143–150 (2011).
23. Beveridge, T. J. & Fyfe, W. S. Metal fixation by bacterial cell walls. *Can J Earth Sci* **22**, 1893–1898 (1985).
24. Ferris, F. G., Fyfe, W. S. & Beveridge, T. J. Bacteria as nucleation sites for authigenic minerals. *Diversity of Environmental Biogeochemistry.* [Berthelin, J. (ed) *Dev. Geochem.* Elsevier, Amsterdam, 319–326, 1991].
25. Zhang, C., Vali, H., Liu, S., Yul, R. & Cole, D. *et al.* in *Instruments, Methods, & Missions for the Investigation of Extraterrestrial Microorganisms* (ed Hoover, R. B.) **3111**, 61–68 (Proc. SPIE, San Diego, CA, USA, 1997).
26. Dupraz, C., Visscher, P. T., Baumgartner, L. K. & Reid, R. P. Microbe–mineral interactions: early carbonate precipitation in a hypersaline lake (Eleuthera Island, Bahamas). *Sedimentology* **51**, 745–765 (2004).
27. Rivadeneyra, M. A., Martín-Algarra, A., Sánchez-Román, M., Sánchez-Navas, A. & Martín-Ramos, J. D. Amorphous Ca-phosphate precursors for Ca-carbonate biominerals mediated by *Chromohalobacter marismortui*. *ISME J.* **4**, 922–932 (2010).
28. Bosak, T. & Newman, D. K. Microbial nucleation of calcium carbonate in the Precambrian. *Geology* **31**, 577–580 (2003).
29. Allwood, A. C. *et al.* "Controls on development and diversity of Early Archean stromatolites." *Proc. Nat. Acad. Sci.* **10**, 9548–9555(2009).
30. Martinez, R. E., Pokrovsky, O. S., Schott, J. & Oelkers, E. H. Surface charge and zeta-potential of metabolically active and dead cyanobacteria. *J. Colloid. Interface Sci.* **323**, 317–325 (2008).
31. Capewell, S. G., Hefter, G. & May, P. M. Potentiometric investigation of the weak association of sodium and carbonate ions at 25°C. *J. Sol. Chem.* **27**, 865–877 (1998).
32. Brown, W. E., Eidelman, N. & Tomazic, B. Octalatium phosphate as a precursor in biomineral formation. *Adv. Dent. Res.* **1**, 306–313 (1987).
33. Brand, U. in *Developments in Sedimentology 51* (eds Chilingarian, V. G. & Wolf, K. H.) 217–282 (Elsevier, Amsterdam, The Netherlands, 1994).
34. Mahamida, J. *et al.* Mapping amorphous calcium phosphate transformation into crystalline mineral from the cell to the bone in zebrafish fin rays. *Proc. Natl. Acad. Sci.* **107**, 6316–6321 (2010).
35. Sánchez-Navas, A. *et al.* in *Advanced Topics on Crystal Growth* (eds Olavo Ferreira, S.) 67–88 (InTech, Croatia, 2013).
36. Bouropoulos, N. Ch. & Koutsoukos, P. G. Spontaneous precipitation of struvite from aqueous solutions. *J. Crys. Growth* **213**, 381–388 (2000).
37. Kofina, A. N. & Kotsoukos, P. G. Spontaneous precipitation of struvite from synthetic wastewater solutions. *Cryst. Growth Des.* **5**, 489–496 (2005).
38. Morse, J. W. The kinetics of calcium carbonate dissolution and precipitation. *Rev. Mineral. Geochem.* **11**, 227–264 (1983).
39. Sánchez-Román, M., Rivadeneyra, M. A., Vasconcelos, C. & McKenzie, J. A. Biomineralization of carbonate and phosphate by moderately halophilic bacteria. *FEMS Microbiol. Ecol.* **61**, 273–284 (2007).

40. Mastandrea, A., Perri, E., Russo, F., Spadafora, A. & Tucker, M. Microbial primary dolomite from a Norian carbonate platform: Northern Calabria, southern Italy. *Sedimentology* **53**, 465–480 (2006).
41. Perri, E. & Tucker, M. Bacterial fossils and microbial dolomite in Triassic stromatolites. *Geology* **35**, 207–210 (2007).
42. Tang, D., Shi, X., Jiang, G. & Zhang, W. Microfabrics in Mesoproterozoic microdigitate stromatolites: evidence of biogenicity and organomineralization at micron and nanometer scales. *PALAIOS* **28**, 178–194 (2013).
43. von der Borch, C. C. & Jones, J. B. Spherular modern dolomite from the Coorong area, South Australia. *Sedimentology* **23**, 587–591 (1976).
44. Benzerara, K. *et al*. Nanoscale detection of organic signatures in carbonate microbiolites. *Proc. Natl. Acad. Sci.* **103**, 9440–9445 (2006).
45. Vasconcelos, C. & McKenzie, J. A. The descent of minerals. *Science* **323**, 218–219 (2009).
46. Schaefer, M. W. Aqueous geochemistry on early Mars. *Geochim. Cosmochim. Acta* **57**, 4619–4625 (1993).
47. Catling, D. C. On Earth, as it is on Mars? *Nature* **429**, 707–708 (2004).
48. Fairen, A., Fernández-Remolar, D., Dohm, J. M., Baker, V. R. & Amils, R. Inhibition of carbonates synthesis in acidic oceans on early Mars. *Nature* **431**, 423–426 (2004).
49. Hurowitz, J. A., Fischer, W. W., Tosca, N. J. & Milliken, R. E. Origin of acidic surface waters and the evolution of atmospheric chemistry on early Mars. *Nature Geoscience* **3**, 323–326 (2010).
50. Hurowitz, J. A. & Woodward Fischer, W. Contrasting styles of water–rock interaction at the Mars Exploration Rover landing sites. *Geochim. Cosmochim. Acta* **127**, 25–38 (2014).
51. Veizer, J., Hoefs, J. Lowe, D. R. & Thurston, P. C. Geochemistry of Precambrian Carbonates: II. Archean greenstone belts and Archean sea water. *Geochim. Cosmochim. Acta* **53**, 859–871 (1989).
52. Morse, J. W. & Mackenzie, F. T. in *Developments in Sedimentology 48* (eds Morse, J. W. & Mackenzie, F. T.) 511–598 (Elsevier, Amsterdam, The Netherlands, 1990).
53. Sumner, D. Y. Carbonate precipitation and oxygen stratification in late Archean seawater as deduced from facies and stratigraphy of the Gamohaan and Frisco formations, Transvaal Supergroup, South Africa. *Am. J. Sci.* **297**, 455–487 (1997).
54. Ohmoto, H., Watanabe, Y. & Kumazawa, K. Evidence from massive siderite beds for a CO2-rich atmosphere before ~1.8 billion years ago. *Nature* **429**, 395–399 (2004).
55. Craddok, P. R. & Dauphas, N. Iron and carbon isotope evidence for microbial iron respiration throughout the Archean. *Earth. Planet. Sci. Lett.* **303**, 121–132 (2011).
56. Schmid, T. *et al.* Tip-enhanced Raman spectroscopy and related techniques in studies of biological materials. *Proc. SPIE* **7586 758603**, 13 pp (2010).
57. Edwards, H. G. M., Moody, C. D., Newton, E. M., Villar, S. E. J. & Russell, M. J. Raman spectroscopic analysis of cyanobacterial colonization of hydromagnesite, a putative martian extremophile. *Icarus* **175**, 372–381 (2005).
58. Schuster, K. C., Reese, I., Urlaub, E., Gapes, J. R. & Lendl, B. Multidimensional Information on the Chemical Composition of Single Bacterial Cells by Confocal Raman Microspectroscopy. *Anal. Chem.* **72**, 223 5529–5534 (2000).
59. Takai, Y., Masuko, T. & Takeuchi, H. Lipid structure of cytotoxic granules in living human killer T lymphocytes studied by Raman microspectroscopy. *Biochim. Biophys, Acta* **1335**, 199–208 (1997).
60. Parkhust, D. L. & Appelo, C. A. J. *User's Guide to PHREEQC, Version 2* (US Geological Survey, Denver, CO, 1999).

Acknowledgments

This work was supported by the European research project ERC-250350/IPBSL. A.S.-N. acknowledges support from the P11-RNM-7067 (Junta de Andalucía-C.E.I.C.-S.G.U.I.T.) project.

Author contributions

M.S.R. designed the culture experiments and performed most of the laboratory tasks, carried out the culture experiments and wrote the first draft of the manuscript. P.S.M. assisted with the design and performance of the culture experiments. A.S.N. and N.R. contributed with SEM and TEM analyses. T.S. performed the AFM and Raman analyses. D.F.R., R.A., C.V. and J.A.M. assisted with the figures and text, and all authors assisted in preparing the manuscript and read and approved the final version.

Additional information

Competing financial interests: The authors declare no competing financial interests.

How to cite this article: Sánchez-Román, M. *et al.* Microbial mediated formation of Fe-carbonate minerals under extreme acidic conditions. *Sci. Rep.* **4**, 4767; DOI:10.1038/srep04767 (2014).